Sulfur isotopes of organic matter preserved in 3.45-billion-year-old stromatolites reveal microbial metabolism

Tomaso R. R. Bontognali[a,1], Alex L. Sessions[a], Abigail C. Allwood[b], Woodward W. Fischer[a], John P. Grotzinger[a], Roger E. Summons[c], and John M. Eiler[a]

[a]Geological and Planetary Sciences, California Institute of Technology, Pasadena, CA 91125; [b]Jet Propulsion Laboratory, California Institute of Technology, Pasadena, CA 91109; and [c]Department of Earth, Atmospheric, and Planetary Sciences, Massachusetts Institute of Technology, Cambridge, MA 02139

The 3.45-billion-year-old Strelley Pool Formation of Western Australia preserves stromatolites that are considered among the oldest evidence for life on Earth. In places of exceptional preservation, these stromatolites contain laminae rich in organic carbon, interpreted as the fossil remains of ancient microbial mats. To better understand the biogeochemistry of these rocks, we performed microscale in situ sulfur isotope measurements of the preserved organic sulfur, including both $\Delta^{33}S$ and $\delta^{34}S_{CDT}$. This approach allows us to tie physiological inference from isotope ratios directly to fossil biomass, providing a means to understand sulfur metabolism that is complimentary to, and independent from, inorganic proxies (e.g., pyrite). $\Delta^{33}S$ values of the kerogen reveal mass-anomalous fractionations expected of the Archean sulfur cycle, whereas $\delta^{34}S_{CDT}$ values show large fractionations at very small spatial scales, including values below $-15‰$. We interpret these isotopic patterns as recording the process of sulfurization of organic matter by H_2S in heterogeneous mat pore-waters influenced by respiratory S metabolism. Positive $\Delta^{33}S$ anomalies suggest that disproportionation of elemental sulfur would have been a prominent microbial process in these communities.

early life | biosignature | microbe | paleontology | ion probe

Putative fossil microorganisms and stromatolites interpreted as fossil microbial mats are considered to be the earliest morphological evidence for the existence of life on Earth (1–3). The simple morphology of these structures makes it very difficult to identify the kind of life that they might represent. More precise information on specific metabolic pathways can be obtained by analyzing the isotopic composition of ancient materials, which may record fractionation indicative of biological processing (4). However, in some specific geological settings, such as hydrothermal systems, isotopic fractionation analogous to that produced by microbes can result from purely abiotic processes (5–7). Thus, in order to avoid any misinterpretations, it is of key importance that isotopic measurements be performed on samples whose depositional setting and geological history are as much as possible constrained and understood. This is the case of the stromatolites present in the *ca*. 3.4–billion-year (Ga)–old Strelley Pool Formation (SPF) of Western Australia, whose petrology and sedimentology have been extensively studied (1, 8–10). These sedimentary structures show a morphologic complexity and diversity that is best explained by involvement of microbial mats in their formation (1). Furthermore, they contain organic material preserved by early silicification, interpreted as the biomass of ancient microbial mats (8). This fossil organic material, whose authigenic and primary origin is supported by petrographic relationships with the stromatolitic laminations (8), offers the opportunity to gain, via isotopic analysis, new insights into the structure and function of early microbial communities.

Experimental Methods

Sulfur Isotope Records of Metabolism. The abundances of stable sulfur isotopes are often useful in documenting past microbial metabolisms because the fractionations imparted by biology are both large and distinctive. Sulfate-reducing bacteria preferentially metabolize ^{32}S relative to ^{34}S, releasing H_2S that is depleted in ^{34}S by up to approximately 70‰ (11, 12). Similar isotopic fractionations are also produced by microbes that disproportionate sulfur compounds of intermediate oxidation state (e.g., S^0, $S_2O_3^{2-}$, and SO_3^{2-}) (13, 14). In natural anaerobic environments, these biologic processes result in dissolved porewater sulfide characterized by relatively low, often variable $\delta^{34}S_{CDT}[= (^{34}S/^{32}S)_{sample}/(^{34}S/^{32}S)_{CDT} - 1]$ values (15) that can be recorded in sedimentary rocks by the precipitation of sulfide-bearing minerals like pyrite. Consequently, large ranges in $\delta^{34}S$ values of sedimentary pyrite are widely used to infer the operation of sulfur-based metabolisms from present day to about 2.5 Ga ago (16, 17).

Older rocks record much lower $\delta^{34}S$ variability, potentially indicating either a lack of sulfur-based metabolism (18) or that such metabolism operated under low seawater sulfate concentrations, where net fractionations are generally small (19). A notable exception to this trend is the observed large range of $\delta^{34}S$ values recorded in discontinuous laminations of microscopic pyrite hosted in large bedded barite crystals from the 3.47-Ga North Pole deposits of northwestern Australia. Those $\delta^{34}S$ values were first interpreted as the earliest evidence for microbial sulfate reduction (MSR) (20), and, in later studies based on ^{33}S and ^{36}S measurements, it was debated whether this isotopic signal is indeed due to MSR or microbial elemental sulfur disproportionation (MSD) (21–23). What is certain, however, is that the petrogenesis of these barite and pyrite samples is unusual, and they may also be a product of abiotic processes (24–26). A recent study measuring sulfur isotope ratios of pyrite preserved within a sandstone of the *ca*. 3.4-Ga SPF arrived at a similar conclusion, that both MSR and MSD were active in the sediments at that time (27). Some of these pyrite crystals are found in the same samples with organic structures interpreted as microfossils, which was used to further support the biological origin of the observed isotopic signal (28).

These ideas are consistent with independent observations from comparative biology suggesting that the biochemistry underpinning these sulfur metabolisms was present early in the history

of life (29). However, it is unclear why such signatures of sulfur metabolism are limited to only a few occurrences in early Archean successions, but then disappear for more than one billion years until Paleoproterozoic time, when large S-isotopic fractionations are again recorded in sedimentary sulfides (16, 30). It is thus reasonable to question the origin of these early Archean pyrite records and whether or not they accurately reflect microbial activities, or might instead reflect fractionations introduced later in the complex history of these sedimentary rocks (31).

To provide insight into this problem, we have measured multiple sulfur isotope ratios preserved in organic matter (kerogen) rather than in pyrite or barite. These are unique data reported for Archean rocks. This archive likely records operation of the sulfur cycle in a slightly different way than does sedimentary pyrite, and offers a metric for comparison. And while the interpretation of organic sulfur (OS) isotope data is no less complex than for pyrite, comparison of these two parallel proxies can improve confidence in their interpretation, especially when observing a suite of rocks that inevitably record a complex history of primary, diagenetic, and metamorphic processes (26). Furthermore, the OS proxy can be mechanistically connected to a sedimentary texture that itself may constitute a biosignature, inherently reinforcing any biological interpretation. Measurement of OS in Archaean rocks is, however, quite challenging and required development of a unique analytical approach.

Ion Probe Measurements of Organic Sulfur. A significant problem in studying OS within Archean rocks is that its relative abundance is typically low, and the organic domains are very small, thermally over-mature, and thus not readily extractable in sufficient amount for conventional bulk analysis. In order to meet this challenge, we developed a method that uses secondary ion mass spectrometry (SIMS) to make OS isotope measurements on small quantities of kerogen obtained by acid extraction, as well as directly in situ on petrographic thin-sections. A Cameca NanoSIMS 50L ion probe was used to perform $\delta^{34}S$ measurements on thin sections and acid extracts from regions of 3×3 µm. In addition, we used a Cameca IMS 7f-GEO, but—due to the more limited spatial resolution of approximately 10×10 µm—exclusively on kerogen extracts.

The analytical performance of this method was documented through analyses of four Phanerozoic kerogen standards of various origin and S/C ratios, with bulk $\delta^{34}S$ values ranging from −23‰ to +27‰ (Table S1). The results obtained with the two ion probes are consistent with those from an elemental analyzer–isotope ratio mass spectrometer (EA-IRMS) and indicate an overall uncertainty in $\delta^{34}S$ of less than 5‰ using either SIMS instrument (Fig. 1 and Tables S1–S4). $\Delta^{33}S$ measurements (where $\Delta^{33}S = \delta^{33}S - 0.515\delta^{34}S$) were only performed on kerogen extracts using the IMS-7f GEO, with a spatial resolution of 50×50 µm and an overall precision of 0.5‰ (Table S3).

$\delta^{34}S$ values do not reflect differences in the S/C ratio of the samples or the sulfur ion count rate (Tables S1–S4), and the measured variability of $\delta^{34}S$ is substantially larger than the expected analytical precision, particularly for in situ analyses with the NanoSIMS instrument. The exact cause of this fine-scale isotopic variability is less clear. Previous ion probe studies targeting pyrite observed microscale isotopic variability and interpreted this to indicate microbial processes (15, 27, 32). It is known that these metabolic processes—and consequently their isotopic fractionations—vary significantly in space and time and as a function of mass flux within the system (i.e., open versus closed system) (14, 27). Thus, a biological origin represents one reasonable interpretation for small-scale isotopic variability observed in the studied kerogens. However, no study has specifically evaluated the isotopic homogeneity of abiotic OS, and ion probe studies of sulfide minerals have shown that small-scale isotopic variability up to 20‰ might also form in hydrothermal settings where a biogenic source of sulfide is not obvious (32). Thus, small-scale
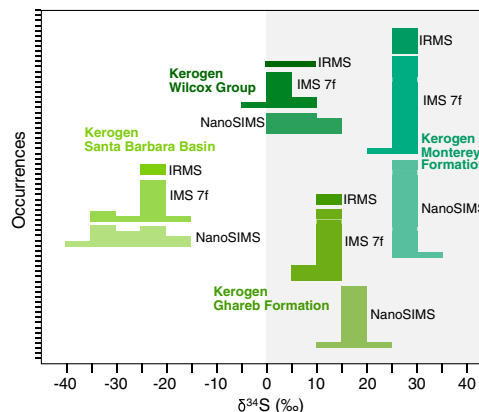

Fig. 1. Comparison of $\delta^{34}S$ measurements of OS using three different analytical techniques. Histograms represent the $\delta^{34}S$ values of four kerogen standards that were measured by EA-IRMS, by magnetic sector SIMS (IMS 7f), and by nanoscale SIMS (NanoSIMS). These analyses demonstrate that the accuracy of the IMS-7f and NanoSIMS is comparable to that of IRMS, a technique that allows better precision but has a spatial resolution limited to bulk samples.

isotopic variability in OS by itself cannot unambiguously prove the existence of past sulfur metabolism. Further observations will be required to ascertain whether such fine-scale isotopic variability is characteristic of biological sulfur cycling.

Geological Context of the Studied Samples. Sediments of the SPF were deposited on the Pilbara Craton, Western Australia, between 3.43 and 3.35 Ga ago (1), and are part of the southwestern Panorama Greenstone Belt. This formation contains the Earth's oldest preserved carbonate platform, including a well-developed stromatolite reef. The present study focuses on samples of encrusting domical stromatolites (8) from a bed near the base of the carbonate platform succession (bed 1 of SPF member 2), collected from an outcrop situated on southern "Anchor Ridge" (8). These stromatolites consist of laminated dolomite and chert with discontinuous layers of carbonaceous material and chert-filled fenestrae (8). Organic matter is preserved in many of the stromatolites and occurs in discrete laminae that are concordant with the carbonate depositional laminae, including intraclast conglomerates that onlap the stromatolites. These organic-rich layers are comprised of silicified organic particles situated along dolomite grain boundaries (Fig. 2), both of which are surrounded by early diagenetic isopachous fenestrae-filling chert and a chert matrix that contains negligible organic matter. These petrographic relationships indicate that organic-rich layers formed at the stromatolite-water interface prior to diagenesis and were not later introduced into the rock (8). Moreover, organic-rich layers adhered to stromatolite slopes steeper than 30°, without thickening into lows as expected if the organic particles were detrital in origin. These textural features indicate that the organic material is syngenetic and autochthonous, and likely reflects the relict biomass of an ancient microbial mat (8). This interpretation is further supported by Raman spectroscopic studies of the various facies within the SPF, showing that the carbonaceous material within the stromatolites has a lower thermal maturity (i.e., approximately 200 °C) compared to the organic carbon in both older and younger deposits of hydrothermal origin that record temperatures of approximately 400 °C (10, 33).

Results

Ion probe measurements of kerogen extracted from the SPF stromatolites by HF/HCl dissolution of the chert matrix revealed a large range of $\delta^{34}S$ values, including some below −15‰ (Fig. 3). Those measured with the IMS-7f from regions of 10×10 µm show a total range of approximately 20‰ with an average value

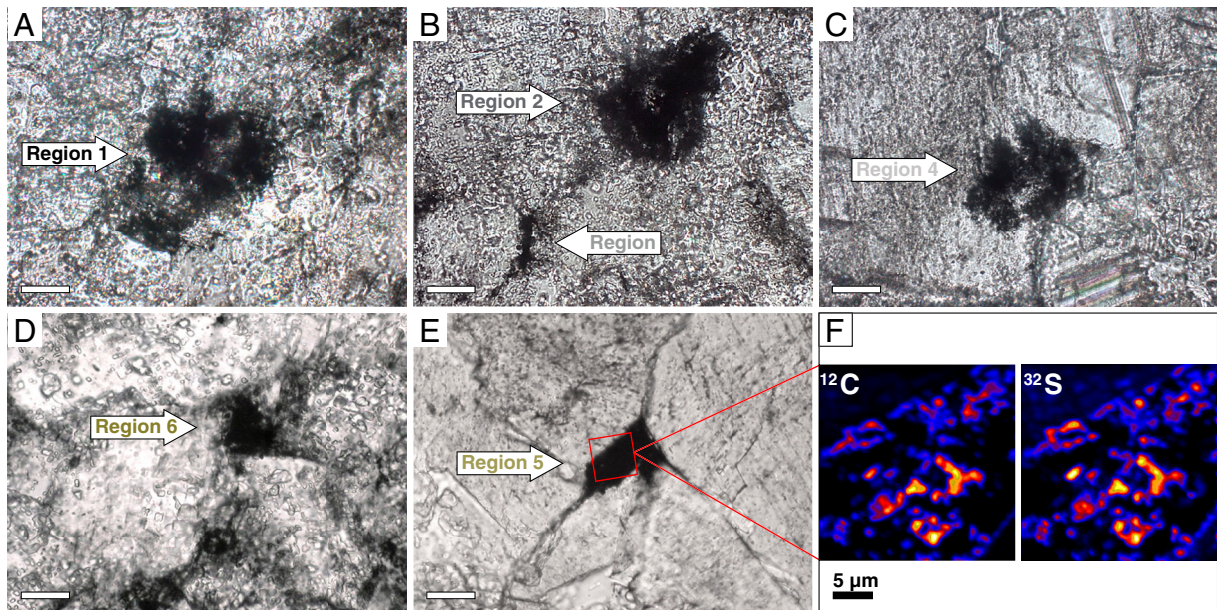EARTH, ATMOSPHERIC, AND PLANETARY SCIENCES

EVOLUTION

Fig. 2. Silicified organic matter preserved in the 3.45-Ga SPF stromatolites. (*A–E*) Transmitted light photomicrographs showing the organic-rich regions analyzed by NanoSIMS. Scale bars, 20 μm. (*F*) NanoSIMS ion maps of ^{12}C and ^{34}S (red square in *E*). The coregistration between the abundance of ^{12}C and ^{34}S in the ion images indicates that measured $\delta^{34}S$ values derive from sulfur incorporated into organic matter. The organic material is finely dispersed within the chert, forming aggregates that rarely exceed a size of 3×3 μm.

of −11.5‰ (Table S2), and $\Delta^{33}S$ values ranging from −0.2 to +2.1‰ (Fig. 3 and Table S3). Those measured by NanoSIMS from regions of 3×3 μm show an even larger range of approximately 40‰ with an average value of −6.7‰ (Fig. 4 and Table S4). The NanoSIMS results are consistent with those made on the IMS-7f within an uncertainty of 5‰, the effective precision defined by measurements of four different kerogen standards (Fig. 1). NanoSIMS analyses were also performed directly in situ on two petrographic thin sections, and include a total of six regions that contain preserved organic material (Figs. 2 and Figs. S1 and S2). Kerogen in each region was also characterized by Raman spectroscopy (Fig. S3). Consistent with previous reports, kerogen in these SPF samples is composed of disordered organic matter that witnessed maximum postdepositional temperatures equivalent to lower greenschist facies metamorphism (10). The maturity of this organic matter matches the expected thermal grade experienced by the host rock (25), and rules out contamination of our samples by modern endolithic bacteria. The $\delta^{34}S$ values of 40 separate organic particles measured in situ

by NanoSIMS range from −17.4‰ to +36.6‰, with an average value of +5.5‰. Differences of more than 30‰ are common between adjacent particles, which are in some cases separated by less than 50 μm. NanoSIMS $\delta^{34}S$ analyses of the extracted kerogen (with bulk $\delta^{13}C$ of −27.8‰) are, on average, slightly more negative than values obtained by in situ measurements performed directly on the stromatolite thin sections (Fig. 3). It is difficult to assess whether these distributions are meaningfully different, or would instead converge given more observations of other regions within the stromatolite. If the distributions are indeed real, several factors might contribute to the difference (see *SI Discussion*). Although it is quite unlikely that the observed offset is due to a matrix effect, which is expected to preferentially increase counts of the lighter isotope and thus lower the isotope ratio (opposite to the observed trend), we cannot rigorously exclude that the presence of the chert matrix has a cryptic effect on our NanoSIMS measurements that is not present in our admixture control experiments.

Rare pyrite crystals were identified in the early-silicified stromatolites, offering an opportunity to compare the isotopic composition of these two different S-bearing phases. These crystals
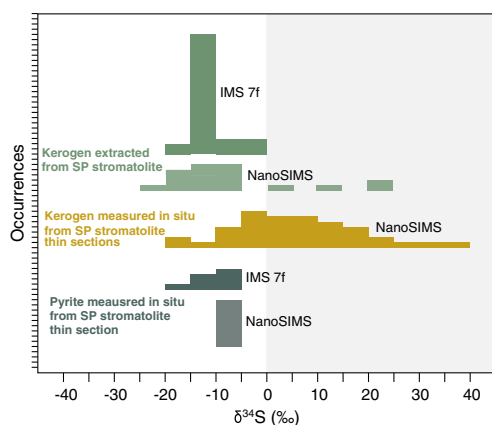

Fig. 3. Sulfur isotopic compositions of kerogen and sulfide minerals present within SPF stromatolites. Histograms represent $\delta^{34}S$ values measured with two ion probes from acid extracts, in situ from six different regions of the stromatolite (Fig. 2), and in situ from pyrite crystals (Fig. S4).
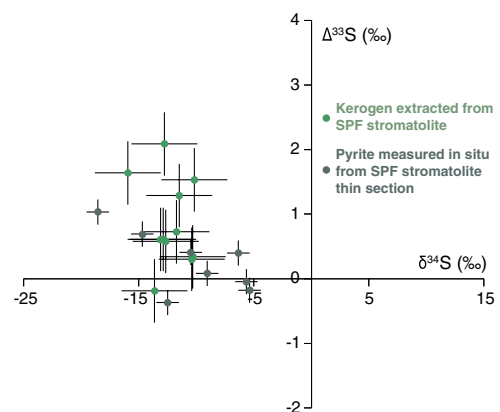

Fig. 4. $\Delta^{33}S$ and $\delta^{34}S$ values (with 1σ error bars) of OS and sulfide minerals present within the SPF stromatolites.

are not spatially associated with the kerogen and show a euhedral habit indicating precipitation during late diagenesis/metamorphism and/or recrystallization of existing pyrites (Fig. S4). IMS-7f and NanoSIMS measurements of these pyrites revealed $\delta^{34}S$ values that range from $-18.6‰$ to $-5.4‰$ (Fig. 3 and Tables S3 and S4) and $\Delta^{33}S$ values ranging from -0.2 to $+1$ (Fig. 4 and Table S3).

$\delta^{34}S$ values measured from pyrite crystals are broadly similar to those measured from isolated kerogens, whereas they are approximately $10‰$ depleted in ^{34}S relative to $\delta^{34}S$ of the in situ OS measurements (Fig. 3). OS in marine sediments is commonly enriched in ^{34}S relative to the coexisting pyrite by an average of 10–$20‰$ (34, 35). The reasons for this offset remain unclear and debated (36). One proposed explanation is that pyrite derives entirely from a reduced sulfur pool, whereas OS also includes a portion of biosulfur assimilated from a sulfate pool enriched in ^{34}S (34). According to this view, and consistent with our data from acid extracts, smaller differences should be expected in the Archean mats wherein fractionations between sulfate and sulfide were likely smaller (19). Timing of the sulfur incorporation, different sulfur species, and fractionation due to the sulfurization process are other factors that might produce isotopic fractionations between OS and pyrite (36). In our case, the absence of a large offset combined with petrographic evidence for pyrite recrystallization makes it difficult to speculate on the relative importance of these processes. It is entirely possible that pyrite formed from H_2S deriving from the thermal maturation of kerogen, which would naturally explain their similar $\delta^{34}S$ values. The $\Delta^{33}S$ values of OS are, on average, slightly more positive than those of pyrite. However, considering the overall range of values recorded in both phases, it would be speculative to propose two substantially different S sources for OS and pyrite. Likely, sulfur constituting the pyrite and that vulcanized into organic matter has the same primary origin, and the local $\delta^{34}S$ differences might be attributed to slightly different times of emplacement and/or slight modification during metamorphism. The crystal habit, $\delta^{34}S$, and $\Delta^{33}S$ values of pyrite crystals present within the SPF stromatolites are similar to those measured in a previous study from member 1 of the formation, which have been interpreted as the product of microbial activity (27).

Discussion

The organic matter in fossil microbial mats from the SPF exhibits a large range in sulfur isotope ratios. In general terms, the isotopic composition of sedimentary OS could depend on (*i*) the isotopic composition of biologically assimilated sulfur, generally from environmental sulfate (34), (*ii*) the isotopic composition of pore water sulfide and polysulfide species undergoing abiotic reactions with organic functional groups (34–36), and (*iii*) isotopic fractionations occurring during thermal maturation of the sedimentary organic matter. The isotopic fractionation associated with assimilatory sulfate reduction is generally small (i.e., approximately 1–3‰) (37); thus, biosulfur has an isotopic composition close to that of ambient sulfate. In modern marine environments, assimilated biosulfur has a $\delta^{34}S$ value of approximately 21‰ reflecting the marine sulfate reservoir. The isotopic composition of seawater sulfate (or other species that might have served for assimilation) in Archean oceans is unknown, but it is likely to have been closer to 0‰.

The isotopic composition of diagenetic OS is determined by that of reactive porewater species, primarily sulfide and polysulfides, due to the fractionation associated with the activities of MSR and MSD. Fractionations associated with the sulfurization process itself are small, with a maximal reported difference of 4–5‰ between porewater sulfide/polysulfides and OS (36). Diagenetic sulfur is thought to account, on average, for at least 80% of the total OS in Phanerozoic sediments (34, 38). In older rocks, the exact contributions of biosulfur and diagenetic sulfur

cannot be easily determined. Diagenetic sulfurization could have been less important if seawater sulfate concentrations—and thus porewater sulfide concentrations—were substantially lower. However, studies of modern sulfate-poor lacustrine environments demonstrate that strictly euxinic conditions are not required for OM sulfurization to take place (39). In some freshwater lakes, significant enrichment of OS has been reported to occur at sulfate concentrations lower than 150 μmol/L, even in the presence of reactive iron (39). Moreover, because the percentage of biosulfur is expected to decrease during diagenesis due to the lability of amino acids, it is likely that OS preserved in mature Archean kerogens mainly derives from sulfurization processes.

Additional modifications of OS can occur as the kerogen thermally matures and ages, but kerogen pyrolysis experiments conducted at 200–365 °C [the same temperature range reached by the SPF stromatolites during metamorphism (10)] have revealed that these fractionations are small; i.e., <3‰ (40). Thus, fractionations associated with assimilatory biotic processes, abiotic sulfurization reactions, and thermal maturation can only account for $\delta^{34}S$ variations of $-5‰$ to 8‰ with respect to ambient environmental sulfur, and do not explain the larger variations observed in the OS of the SPF stromatolites. Rather, the large variations in $\delta^{34}S$ for kerogen sulfur likely indicate similarly large variations in the composition of environmental sulfate and/or sulfide.

In principle, it is possible for large (tens of permil) variations in $\delta^{34}S$ to result from purely abiotic geological processes; e.g., during hydrolysis of SO_2 in relatively oxidizing magmatic fluids (5) or hydrothermal sulfate reduction in the presence of a metal catalyst (6). However, the petrographic context of the samples studied here does not support a hydrothermal origin of the kerogen. Rather, early silicification of host stromatolites appears to have provided the unique taphonomic window for preservation of the former mats. Rare earth element distributions in member 2 of the SPF, which include the studied stromatolites, indicate that chert and carbonate present in association with kerogen was derived from seawater, and that neither appear to be replacement phases derived from hydrothermal fluids that may have impacted the SPF elsewhere (9).

Anomalous mass dependence of sulfur isotope ratios (i.e., $\Delta^{33}S \neq 0$) are common in many sulfide and sulfate minerals older than 2.4 Ga, but are virtually absent in younger rocks (41). These anomalies have been interpreted as the result of gas-phase reactions that occurred in an early anoxic atmosphere before the great oxidation event (41). SO_2 photolysis causes isotopic mass-independent fractionation (MIF), forming elemental sulfur with positive $\Delta^{33}S$ anomalies and sulfate with negative anomalies (41, 42). In the absence of oxidative homogenization, such signals might be independently transferred from the atmosphere to the oceans and then preserved in the rock record (43, 44). According to this hypothesis, the presence of a positive $\Delta^{33}S$ anomaly in the kerogen extracted from the SPF stromatolites further confirm its Archean origin, indicating that at least part of the vulcanized sulfur derived from aerosols produced in an early anoxic atmosphere.

Concurrent with MIF, photolytic reactions also produce conventional mass-dependent fractionations (42). Positive correlations between $\Delta^{33}S$ anomalies and $\delta^{34}S$ values recorded in pyrites have been interpreted to represent a photolytic signal, without further modification by other fractionation processes (45). Such a correlation is not observed in the SPF stromatolites (Fig. 4); thus, the observed $\delta^{34}S$ values cannot be explained exclusively through atmospheric reactions. An additional fractionating process must have overprinted the photolytic signal. In studies targeting pyrites, positive $\Delta^{33}S$ anomalies associated with negative $\delta^{34}S$ values (as observed in the SPF kerogen) are interpreted to have formed via microbial disproportionation of the elemental sulfur reservoir, whereas microbial reduction of sulfate should produce negative $\delta^{34}S$ values and negative $\Delta^{33}S$

anomalies (21, 22, 46). The utility of this interpretative framework is, however, still debated (31, 47). Recent studies have shown that Δ^{33}S anomalies are not exclusively produced in the atmosphere but may also be the result of reactions involving sulfur compounds and organic materials (31, 47). Thus, an unequivocal interpretation of Δ^{33}S values recorded in ancient organic matter will require a better understanding of the processes underlying MIF.

Petrographic relationships and Raman spectroscopy indicate that the analyzed kerogen is autochthonous and was not later introduced into the stromatolite, and the observed Δ^{33}S anomaly (absent in rocks younger than 2.4 Ga) supports the Archean age of the vulcanized sulfur. However, we cannot categorically exclude postburial incorporation of the OS. Fluids produced at distance from the stromatolites could have interacted with the kerogen during burial diagenesis or metamorphism. Nevertheless, sulfide incorporation into the kerogen is considered an important step for the preservation of organic material (38). The affinity of organic matter for sulfide addition is high during early diagenesis, but drops rapidly as functional groups are lost. Thus, it is more likely that sulfide incorporation into the kerogen occurred during early diagenesis, rather than substantially later during metamorphism of a silicified rock.

Taken together, these results suggest that organic-rich laminae within the SPF stromatolites contain sulfur that was derived from porewater sulfide present in an ancient microbial mat during the deposition of primary sediments. The abundant positive Δ^{33}S anomalies recorded in OS indicates that the ultimate source of sulfur was predominantly atmospherically cycled elemental sulfur. In order to be incorporated into kerogen, elemental sulfur would first have to be reduced to sulfide or polysulfide. We propose that such a transformation was achieved by sulfur disproportionating organisms, using organic compounds (for example the biomass of SPF mats), H_2, or CH_4 as electron donors to form H_2S. This microbial process is known to induce significant S-isotopic fractionation, and can explain the negative δ^{34}S values recorded in OS. Conversely, negative δ^{34}S values of OS are very difficult to explain as deriving largely from bioassimilated seawater sulfate. Indeed, assimilatory processes do not produce large isotopic fractionations, and, in the Archean, seawater sulfate likely had an isotopic composition close to $0‰$ (17). Our data do not exclude additional sulfur processing by MSR, which could have coexisted with MSD. Mixing between sulfate deriving from the atmosphere and sulfate produced by MSD (characterized by Δ^{33}S values of opposite sign) may have caused dilution and homogenization of the negative anomaly that is usually attributed to MSR (21, 43).

δ^{34}S patterns similar to that recorded in the SPF stromatolites are known from modern microbial mats of Guerrero Negro, Mexico (15). This study, also using NanoSIMS, examined the isotopic composition of dissolved HS$^-$ within one such mat and revealed δ^{34}S values as low as $-30‰$, with a range of values greater than $30‰$. These patterns were interpreted as heterogeneous contributions of both MSR and MSD at depth in the microbial mats. We hypothesize that a similar set of processes was responsible for creating the OS we observed in the ca. 3.45 SPF stromatolites.

Our observations provide additional evidence that sulfur-based metabolism was important in ancient Earth surface environments, supporting existing hypotheses derived from pyrite-based studies (20–23, 27, 28, 46, 48, 49). More specifically, we can tie these physiological processes directly to the mats that were part of the stromatolite reefs preserved in the SPF, thus largely circumventing questions about the timing of pyrite formation. This association does not imply or prove that the stromatolitic laminations were formed by S-metabolizing microbes [sensu Grotzinger and Knoll (2)], though it does highlight possible similarities between these early ecosystems and their modern counterparts (50). Sulfur-respiring microbes are commonly found at depth within modern microbial mats, and—in some lithifying mats—they play an important role in forming laminations, both by locally increasing alkalinity and by releasing or degrading exopolymeric substances that promote the precipitation of authigenic minerals (50). Similar biological processes might have contributed to the formation of the SPF stromatolitic reef.

Materials and Methods

SPF stromatolite samples were collected from an outcrop located on southern Anchor Ridge in the northern Pilbara Craton, Western Australia. The exact location of the outcrop and its stratigraphic position are described in detail by ref. 8. Bulk organic matter was isolated from the stromatolites by HF/HCl demineralization. Ion probe measurements were performed using a Cameca NanoSIMS 50L and a Cameca 7f-GEO at the Caltech Center for Microanalysis, Pasadena, CA. Ion probe analyses were carried out in situ on ultrapolished thin sections as well as on the isolated kerogen mounted into a layer of indium metal. For detailed information on sample preparation, acid demineralization procedure, kerogen standards, and ion probes analytical conditions see *SI Text*.

1. Allwood AC, Walter MR, Kamber BS, Marshall CP, Burch IW (2006) Stromatolite reef from the Early Archaean era of Australia. *Nature* 441:714–718.
2. Grotzinger JP, Knoll AH (1999) Stromatolites in Precambrian environments: Evolutionary mileposts or environmental dipsticks? *Annu Rev Earth Planet Sci* 27:313–358.
3. Knoll AH (2012) The fossil record of microbial life. *Fundamentals of Geobiology* (Wiley, New York), pp 297–314.
4. Johnston DT, Fischer WW (2012) Stable isotope geobiology. *Fundamentals of Geobiology* (Wiley, New York), pp 250–268.
5. Hattori K, Cameron EM (1986) Archaean magmatic sulphate. *Nature* 319:45–47.
6. Ohmoto H, Goldhaber MB (1997) Sulfur and carbon isotopes. *Geochemistry of Hydrothermal Ore Deposits*, ed HL Barnes (Wiley, New York), pp 517–611.
7. McCollom TM, Seewald JS (2006) Carbon isotope composition of organic compounds produced by abiotic synthesis under hydrothermal conditions. *Earth Planet Sci Lett* 243:74–84.
8. Allwood AC, et al. (2009) Controls on development and diversity of Early Archean stromatolites. *Proc Natl Acad Sci USA* 106:9548–9555.
9. Allwood AC, Kamber BS, Walter MR, Burch IW, Kanik I (2010) Trace elements record depositional history of an Early Archean stromatolitic carbonate platform. *Chem Geol* 270:148–163.
10. Allwood AC, Walter MR, Marshall CP (2006) Raman spectroscopy reveals thermal palaeoenvironments of c. 3.5 billion-year-old organic matter. *Vib Spectrosc* 41:190–197.
11. Harrison AG, Thode HG (1958) Mechanisms of the bacterial reduction of sulfate from isotope fractiontion studies. *Trans Faraday Soc* 53:84–92.
12. Sim MS, Bosak T, Ono S (2011) Large sulfur isotope fractionation does not require disproportionation. *Science* 333:74–77.
13. Bak F, Pfennig N (1987) Chemolithotrophic growth of Desulfovibrio sulfodismutans sp. nov. by disproportionation of inorganic sulfur compounds. *Arch Microbiol* 147:184–189.
14. Canfield DE (2001) Biogeochemistry of sulfur isotopes. *Rev Mineral Geochem* 43:607–636.
15. Fike DA, Gammon CL, Ziebis W, Orphan VJ (2008) Micron-scale mapping of sulfur cycling across the oxycline of a cyanobacterial mat: a paired nanoSIMS and CARD-FISH approach. *ISME J* 2:749–759.
16. Cameron EM (1982) Sulphate and sulphate reduction in early Precambrian oceans. *Nature* 296:145–148.
17. Canfield DE (1998) A new model for Proterozoic ocean chemistry. *Nature* 396:450–453.
18. Canfield DE, Habicht KS, Thamdrup B (2000) The Archean sulfur cycle and the early history of atmospheric oxygen. *Science* 288:658–661.
19. Habicht KS, Gade M, Thamdrup B, Berg P, Canfield DE (2002) Calibration of sulfate levels in the Archean ocean. *Science* 298:2372–2374.
20. Shen Y, Buick R, Canfield DE (2001) Isotopic evidence for microbial sulphate reduction in the early Archaean era. *Nature* 410:77–81.
21. Philippot P, et al. (2007) Early Archaean microorganisms preferred elemental sulfur, not sulfate. *Science* 317:1534–1537.
22. Shen Y, Farquhar J, Masterson A, Kaufman AJ, Buick R (2009) Evaluating the role of microbial sulfate reduction in the early Archean using quadruple isotope systematics. *Earth Planet Sci Lett* 279:383–391.

23. Ueno Y, Ono S, Rumble D, Maruyama S (2008) Quadruple sulfur isotope analysis of ca. 3.5 Ga Dresser Formation: New evidence for microbial sulfate reduction in the early Archean. *Geochim Cosmochim Acta* 72:5675–5691.

24. Van Kranendonk MJ (2006) Volcanic degassing, hydrothermal circulation and the flourishing of early life on Earth: A review of the evidence from c. 3490–3240 Ma rocks of the Pilbara Supergroup, Pilbara Craton, Western Australia. *Earth Sci Rev* 74:197–240.

25. Van Kranendonk MJ, Hickman AH, Smithies RH, Nelson DR (2002) Geology and tectonic evolution of the Archean North Pilbara Terrain, Pilbara Craton, Western Australia. *Econ Geol* 97:695–732.

26. Van Kranendonk MJ, Philippot P, Lepot K, Bodorkos S, Pirajno F (2008) Geological setting of Earth's oldest fossils in the ca. 3.5 Ga Dresser Formation, Pilbara Craton, Western Australia. *Precambrian Res* 167:93–124.

27. Wacey D, McLoughlin N, Whitehouse MJ, Kilburn MR (2010) Two coexisting sulfur metabolisms in a ca. 3400 Ma sandstone. *Geology* 38:1115–1118.

28. Wacey D, Kilburn MR, Saunders M, Cliff J, Brasier MD (2011) Microfossils of sulphur-metabolizing cells in 3.4-billion-year-old rocks of Western Australia. *Nat Geosci* 4:698–702.

29. Meyer B, Kuever J (2007) Phylogeny of the alpha and beta subunits of the dissimilatory adenosine-5′-phosphosulfate (APS) reductase from sulfate-reducing prokaryotes—Origin and evolution of the dissimilatory sulfate-reduction pathway. *Microbiology* 153:2026–2044.

30. Johnston DT (2011) Multiple sulfur isotopes and the evolution of Earth's surface sulfur cycle. *Earth Sci Rev* 106:161–183.

31. Watanabe Y, Farquhar J, Ohmoto H (2009) Anomalous fractionations of sulfur isotopes during thermochemical sulfate reduction. *Science* 324:370–373.

32. McKibben MA, Riciputi LR (1998) Sulfur isotopes by ion microprobe. *Applications of Microanalytical Techniques to Understanding Mineralizing Processes,* eds M McKibben, WC Shanks, III, and WI Ridley*Reviews in Economic Geology* (Shaffer Parkway, Littleton, CO), Vol 7, pp 121–139.

33. Marshall CP, et al. (2007) Structural characterization of kerogen in 3.4 Ga Archaean cherts from the Pilbara Craton, Western Australia. *Precambrian Res* 155:1–23.

34. Anderson TF, Pratt LM (1995) Isotopic evidence for the origin of organic sulfur and elemental sulfur in marine sediments. *Geochemical Transformations of Sedimentary-Sulfur* (American Chemical Society, Washington, DC), pp 378–396 ACS Symposium Series.

35. Werne JP, Lyons TW, Hollander DJ, Formolo MJ, Sinninghe Damsté JS (2003) Reduced sulfur in euxinic sediments of the Cariaco Basin: Sulfur isotope constraints on organic sulfur formation. *Chem Geol* 195:159–179.

36. Amrani A, Aizenshtat Z (2004) Mechanisms of sulfur introduction chemically controlled: δ^{34}S imprint. *Org Geochem* 35:1319–1336.

37. Trust BA, Fry B (1992) Stable sulphur isotopes in plants: A review. *Plant Cell Environ* 15:1105–1110.

38. Werne JP, et al. (2008) Investigating pathways of diagenetic organic matter sulfurization using compound-specific sulfur isotope analysis. *Geochim Cosmochim Acta* 72:3489–3502.

39. Urban NR, Ernst K, Bernasconi S (1999) Addition of sulfur to organic matter during early diagenesis of lake sediments. *Geochim Cosmochim Acta* 63:837–853.

40. Amrani A, Lewan MD, Aizenshtat Z (2005) Stable sulfur isotope partitioning during simulated petroleum formation as determined by hydrous pyrolysis of Ghareb Limestone, Israel. *Geochim Cosmochim Acta* 69:5317–5331.

41. Farquhar J, Bao H, Thiemens M (2000) Atmospheric influence of Earth's earliest sulfur cycle. *Science* 289:756–758.

42. Farquhar J, Savarino J, Airieau S, Thiemens MH (2001) Observation of wavelength-sensitive mass-independent sulfur isotope effects during SO2 photolysis: Implications for the early atmosphere. *J Geophys Res* 106:32829–32839.

43. Halevy I, Johnston DT, Schrag DP (2010) Explaining the structure of the Archean mass-independent sulfur isotope record. *Science* 329:204–207.

44. Pavlov AA, Kasting JF (2002) Mass-independent fractionation of sulfur isotopes in Archean sediments: Strong evidence for an anoxic Archean atmosphere. *Astrobiology* 2:27–41.

45. Ono S, et al. (2003) New insights into Archean sulfur cycle from mass-independent sulfur isotope records from the Hamersley Basin, Australia. *Earth Planet Sci Lett* 213:15–30.

46. Ono S, Beukes NJ, Rumble D (2009) Origin of two distinct multiple-sulfur isotope compositions of pyrite in the 2.5 Ga Klein Naute Formation, Griqualand West Basin, South Africa. *Precambrian Res* 169:48–57.

47. Kopf S, Ono S (2012) Sulfur mass-independent fractionation in liquid phase chemistry: UV photolysis of phenacylphenylsulfone as a case study. *Geochim Cosmochim Acta* 85:160–169.

48. Ohmoto H, Kakegawa T, Lowe DR (1993) 3.4-Billion-year-old biogenic pyrites from Barberton, South Africa: Sulfur isotope evidence. *Science* 262:555–557.

49. Shen Y, Buick R (2004) The antiquity of microbial sulfate reduction. *Earth Sci Rev* 64:243–272.

50. Dupraz C, et al. (2009) Processes of carbonate precipitation in modern microbial mats. *Earth Sci Rev* 96:141–162.

EARTH, ATMOSPHERIC, AND PLANETARY SCIENCES

EVOLUTION